Nitrogen removal in a two-chambered microbial fuel cell: establishment of a nitrifying-denitrifying microbial community on an intermittent aerated cathode.

A. Sotres[1], M. Cerrillo[1], M. Viñas[1] and A. Bonmatí[1*].

[1] IRTA, GIRO Joint Research Unit IRTA-UPC, Torre Marimon, ctra. C-59, km 12,1. E-08140 Caldes de Montbui, Barcelona, Spain.

e-mail addresses: ana.sotres@irta.cat (A. Sotres); miriam.cerrillo@irta.cat (M. Cerrillo); marc.vinas@irta.cat (M. Viñas); august.bonmati@irta.cat (A. Bonmatí).

Abstract

A Microbial fuel Cell (MFC) was used to study nitrogen dynamics and its feasibility for high strength wastewater treatment. Intermittent aeration was applied on the cathode chamber accomplishing the establishment of a simultaneous nitrifying-denitrifying microbial community. A total of 30.4% of the N-NH_4^+ migrated through the ion exchange membrane being primarily nitrified at the cathode chamber. When intermittent aeration was applied in the cathode, denitrification also occurred achieving 17.8% of nitrate removal without acetate addition, and 41.2% with acetate addition. The microbial community analysis revealed that the nitrification process at the cathode chamber could be explained due to a high predominance of *Nitrosomonas* sp. as ammonia-oxidizing bacteria and other *Comamonadaceae* phylotypes as potential denitrifiers. Parallel batch denitrification assays, carried out outside the MFC using the cathode effluent, confirmed the existence of

* Corresponding author. Address: IRTA, GIRO Joint Research Unit IRTA-UPC, Torre Marimon, ctra. C-59, km 12,1. E-08140 Caldes de Montbui, Barcelona, Spain. Tel.: +34 902 789 449 ;Fax. +34 938 650 954 .

heterotrophic denitrification processes with other well known denitrifying dominant phylotypes enrichment (*Burkholderiadaceae*, *Comamonadaceae*, *Alcaligenaceae*).

Keywords: Microbial fuel cell, Ammonia nitrogen migration, Cathodic nitrification-denitrification, 454-pyrosequencing, qPCR.

1. INTRODUCTION

Nitrogen removal from wastewater is increasingly becoming more relevant as a cause for serious environmental problems such as eutrophication of rivers, the deterioration of water sources, and as a serious hazard for human and animal health [1]. Ammonia (NH_3), ammonium (NH_4^+), nitrite (NO_2^-) and nitrate (NO_3^-) are the most important forms of reactive nitrogen found in the environment, and nitrate in particular (NO_3^-), is one of the most problematic compounds found in water and wastewater. Therefore, efforts to improve the removal of nitrogen have intensified in the last decades. Nitrification/denitrification is a well known process applied to remove nitrogen from wastewaters. Nevertheless, as different microbial populations are involved with different requirements of oxygen, temperature, etc., it is often fairly complicated and expensive to implement. Finding new treatment methods to achieve an effective and less expensive nitrogen removal is still an issue to be adequately solved.

Bioelectrochemical systems (BESs) offer a promising technology for nutrient removal while at the same time recovering bioenergy [2]. These systems are capable of converting the chemical energy of organic wastes into electricity. Among all BES, microbial fuel cells (MFCs) are the most widely researched. Microbial fuel cells (MFC) use bacteria as catalysts to oxidize organic and inorganic matter and generate electrical currents since the electrons derived from these metabolic reactions are transferred from the anode (negative terminal) to the cathode (positive terminal) producing a current flow running through an external circuit [3]. A two-chamber MFC, consisting of an anode and a cathode separated by an ion exchange

membrane, is the most common configuration found where, at least one of the anodic or cathodic reactions, is microbiologically catalysed [4].

So far, nitrogen removal by MFCs has focused on two different strategies – MFC ammonium removal under anaerobic conditions [5] or, since that ammonia can be diffused from anode to cathode through the cation exchange membrane [6], it can be stripped and subsequently absorbed [7]. Instead of recovering ammonia at the cathode chamber, another strategy is to remove it by external nitrification and a subsequent denitrification accomplished by microorganisms in the cathode chamber [8,9], or by simultaneous cathodic nitrification-denitrification [10]. So far very few studies referring to nitrogen removal via simultaneous nitrification and denitrification (SND) processes as an alternative of using an external nitrifying bioreactor, which is known to be more difficult and expensive to scale up, have been reported. Afterwards, to simplify the reactor structure and reduce the costs associated caused by using an external nitrifying bioreactor, others MFC designs were investigated in order to carry out SND in these systems. However, to date majority of studies are performed using groundwater or synthetic wastewater, and to contrary the use of high strength animal wastewater, particularly pig slurries, has received little attention so far. Thus, there is a lack of knowledge about the feasibility of using a MFC-SND, and its potential application for treating high strength animal wastewater to accomplish the requirements for agricultural uses.

Nitrification is the biological oxidation of ammonia (NH_4^+) to nitrite (NO_2^-) and then to nitrate (NO_3^-) (equation 1). It is an aerobic process performed by autotrophic ammonia-oxidizing bacteria (AOB), ammonia-oxidizing archaea (AOA) and nitrite-oxidizing bacteria (NOB). The first step of nitrification is the oxidation of ammonia to nitrite catalysed by bacteria containing the ammonia monooxygenase enzyme (*amo*A), being the most studied AOB belonging to the genera *Nitrosomonas*, *Nitrosococcus*, *Nitrosospira* and *Nitrosolobus*. There is less information about AOA, but currently two genera, *Nitrosopumilus* and

Nitrososphaera, have been isolated. The second step is the oxidation of nitrite to nitrate catalysed by bacteria containing the nitrite oxidoreductase enzyme (*nxr*) such as bacteria belonging to the genera *Nitrobacter*, *Nitrococcus*, *Nitrospina*, and *Nitrospira*. Denitrification is an anaerobic respiration pathway for diverse facultative anaerobic bacteria and archaea [11]. It is a sequencing reductive process which involves four steps, from nitrate (NO_3^-) to nitrite (NO_2^-), nitric oxide (NO), nitrous oxide (N_2O) and finally resulting in the production of di-nitrogen gas (N_2) (equation 1). The reduction of nitrous oxide that occurs during the last step of the denitrification pathway involves the *nosZ* enzyme (encoding nitrous oxide reductase), which has received most of the attention in molecular microbial ecology studies in the environment [12]. Heterotrophic bacteria, such as *Paracoccus* and *Pseudomonas*, are the most common denitrifier bacteria, although autotrophic denitrifiers (e.g. *Thiobacillus*) have also been identified.

$$\underbrace{NH_4^+ \xrightarrow{amoA} NO_2^- \xrightarrow{nxr} NO_3^-}_{\text{Nitrification}} \underbrace{\xrightarrow[narG]{napA} NO_2^- \xrightarrow[nirS]{nirK} NO \xrightarrow[norZ]{norB} N_2O \xrightarrow{nosZ} N_2}_{\text{Denitrification}} \quad \text{equation 1}$$

Previous studies focussing on microbial communities' enrichment on bio-cathodes have shown a predominance of members belonging to *Proteobacteria*, *Firmicutes*, and *Chloroflexi* phyla [13]. Taking into account the non-correspondence between changes in predominant microbial populations on the MFC and the reactor's performance, the complex bacteria community harboured on MFCs electrodes, and the fact that occasionally changes in the predominant members of the bacterial community did not correspond with changes in reactor operation [13], it is suggested that more information about functional groups is needed for a better understanding on potential nitrogen transformation mechanisms that could take place in a MFC fed with wastewater.

This study aims to evaluate nitrogen dynamics and microbial community structure in a two-chamber microbial fuel cell operating with an intermittently aerated cathode, and its feasibility as a treatment for high strength (organic and nitrogen) wastewater simulating a liquid fraction of pig slurry. This work focuses on three main goals: i) to study nitrogen dynamics in a MFC harbouring active microbial biomass both in the anode and cathode chambers; ii) to enhance the nitrification-denitrification process at the cathode chamber, and iii) to assess the microbial community enriched both in the cathode compartment and in the anode.

2. MATERIALS AND METHODS

2.1 Experimental set-up

A methacrylate two-chambered MFC reactor was built with the anode and cathode compartments (0.14 x 0.12 x 0.02 m^3) separated by a cation exchange membrane (CEM) (14x12 cm) (Ultrex CMI-7000, Membranes International Inc., Ringwood, NJ, USA). Granular graphite rods with a diameter ranging from 2 to 6 mm (El Carb 100, Graphite Sales Inc., U.S.A.), and stainless steel mesh were used as anode and cathode respectively, resting in 165 mL of net anodic volume (NAV) and 250 mL of net cathodic volume (NCV). Prior to its use, the granular graphite was sequentially soaked in 1M of HCL, and 1M of NaOH, in each case for 24 hours, and finally rinsed in deionised water. Copper wires were used to connect the electrodes to a 500 Ω external resistance.

2.2 MFC operation

The anodic chamber was inoculated with 1 mL of digestate from a bench-scale mesophilic methanogenic continuously stirred tank reactor fed with slaughterhouse waste harbouring a high content of $N\text{-}NH_4^+$.

The feed solutions were prepared containing (distilled water): $CaCl_2$, 0.0147 g; KH_2PO_4, 3 g; Na_2HPO_4, 6 g; $MgSO_4$, 0.246 g; and 1 mL L^{-1} trace elements solution as described in Lu et al. [14]. Additionally the anode feed solution contained 2.9 g L^{-1} CH_3COONa, as carbon source, and 3.82 g L^{-1} NH_4Cl; accordingly, the COD:N ratio of the medium was 2.23. The feed solution for the cathode chamber contained KH_2PO_4, 3 g L^{-1}; Na_2HPO_4, 6 g L^{-1}. The MFC was operated at a room temperature of ~ 23 ºC and in a continuous mode with a flow rate of 0.628 L d^{-1}, resulting in organic and nitrogen loading rates of 1.7 g COD L^{-1} d^{-1} and 4.2 g N-NH_4^+ L^{-1} d^{-1} respectively. The operated hydraulic retention time (HRT) was of 6.3 and 9.4 h at the anode and cathode respectively (Table 1). To keep the cathode under aerobic conditions, air was supplied at a flow rate of 2 L min^{-1}. Then, a side batch assay, as described in point 2.3, was performed to assess the occurrence of denitrification biomass in the cathode. Finally, in order to accomplish our second objective, three different cathode aeration patterns were carried out: (i) short intermittent aerated periods (P. 2.1), followed by (ii) long intermittent aerated periods (P. 2.2), and (iii) long intermittent aerated periods plus acetate addition (P. 2.3). Samples were taken from the anode and the cathode compartment three times a day during the continuous cathode aeration period (P. 1), and during the intermittent aeration, before and after each different aerated period (P. 2.1, 2.2 and 2.3).

2.3 Denitrification batch assays

Denitrification batch assays were carried out to confirm the presence of denitrifiers on the MFC cathode. Glass vials of 120 mL volume were filled with 60 mL of cathode effluent and different carbon sources and a potential denitrifying inocula. Four experimental conditions were studied: (i) the cathode effluent, (ii) the cathode effluent plus acetate, (iii) the cathode effluent plus the anode effluent, and iv) a negative control (autoclaved cathode effluent).

To create anaerobic conditions, oxygen was removed bubbling up each bottle with N_2 for 10 minutes. All conditions were carried out per triplicate and, to avoid substrate limitations,

COD in condition (ii) was added in excess. Batch assays lasted 160 h, and samples were taken every 24 hours.

2.4 Electrochemical analysis

Voltage (*V*) across the external resistance (Ω) was recorded at 20 min intervals using a multimeter data acquisition unit (Mod. 34970A, Agilent Technologies, Loveland, CO, USA). The current density (*I*) was then calculated using Ohm´s Law, and the power density (*P*) was obtained using $P = IV/A$, where *I* stands for current density (mA), *V* stands for the voltage (mV), *A* stands for the cell volume (m^3) and *P* stands for the power density ($mW\ m^{-3}$).

Polarization curves (*P* versus *I*) were carried out in order to obtain the maximum power density and the internal resistance of the system. The procedure to obtain a polarization curve was set up as follows: after leaving the system in open circuit for 1 hour, the circuit was closed and the external resistance was changed from 20000 to 10 Ω (20000, 10000, 2200, 1000, 500, 100, 50 and 10). Upon the connection of each resistance, the system was left to stabilize for 30 min before recording the voltage data.

2.5 Chemical analysis and calculations

Ammonium NH_4^+-N, nitrate NO_3^--N, nitrite NO_2^--N, pH, and soluble COD were analysed according to Standard Method 5220 [15]. Nitrate (NO_3^--N) and nitrite (NO_2^--N) concentrations were analysed by ion chromatography (Metrohm 861 Advanced Compact IC), using a Metrohm Metrosep A Supp 4 column and pre-column, a Metrosep A Supp 4/5 Guard with 1.8 mmol $NaCO_3$/L, and 1.7 mmol $NaHCO_3$/L effluent once filtered through a 0.2 µm pore diameter PTFE syringe filter (VWR International, LLC.). Ammonium (NH_4^+-N) was analysed using a Büchi B-324 distiller, and a Metrohm 702 SM autotitrator. The bulk solution pH in each experiment was tested using a CRISON 2000 pH electrode. Soluble COD was measured following an optimized APHA−AWWA−WPCF Standard Method and filtering the samples through a 0.45 µm pore diameter Nylon syringe filter (Scharlau, S.L.).

Total nitrogen (TN) was defined as the sum of ammonium (NH_4^+-N), nitrite (NO_2^--N), and nitrate (NO_3^--N) concentrations. And the total nitrogen and nitrate removal efficiency, η_{TN} and η_{NO3^-N} respectively, was calculated based on the difference between initial and final concentrations in the bulk solution at the beginning and at the end of every sampling period divided by its initial concentration.

Coulombic efficiency (*CE*), defined as the ratio of electrons used as current to the theoretical maximum electron production, was calculated as described elsewhere [3].

2.6 Microbial community analysis

Samples from each of the experiments were taken and analysed using different culture-independent techniques such as the *16S rRNA* gene-based PCR-DGGE, and 454-Pyrosequencing, as well as real time PCR (qPCR) for the *16S rRNA* gene and two other functional genes (*amoA* and *nosZ*) in order to gain insight on the microbial community structure.

2.6.1 Denaturing gradient gel electrophoresis (DGGE)

The bacterial communities enriched on the anode and cathode chambers of the MFC were analysed by means of DGGE. Total DNA was extracted in triplicate from known volumes/weights of each sample with the PowerSoil® DNA Isolation Kit (MoBio Laboratories Inc., Carlsbad, CA, USA), following the manufacturer's instructions. Universal eubacterial forward (F341) and reverse (R907) primers were used to amplify the hypervariable (V3-V5) region of the *16S rRNA* gene by a polymerase chain reaction (PCR), as previously reported [16] (Table 2). All PCR reactions were carried out in a Mastercycler (Eppendorf, Hamburg, Germany) and each reaction mix (25 μL mix/reaction) contained 1.25 U of Ex TaqDNA polymerase (Takara Bio Inc., Otsu, Shiga, Japan), 12.5 mM dNTPs, 0.25 μM of each primer, and 100 ng of DNA.

The PCR amplicons (20 µL) were loaded in an 8% (w/v) polyacrylamide gel (0.75 mm thick) with a chemical denaturing gradient ranging from 30% to 70% (100% denaturant stock solution contained 7 M urea and 40% (w/v) of formamide).

The electrophoresis was carried out in a DGGE-4001 system (CBS Scientific Company Inc., Del Mar, CA, USA) at 100 V and 60 °C for 16 h in a 1x TAE buffer solution (40 mMTris, 20 mM sodium acetate, 1 mM EDTA, pH 7.4). The DGGE gels were stained in darkness for 45 min with 15 mL of a 1x TAE buffer solution containing 3 µL of SYBR® Gold 10,000x (Molecular Probes, Eugene, OR, USA). The gels were scanned under blue light by means of a blue converter plate (UV Products Ltd., Cambridge, UK) and a transilluminator (GeneFlash, Synoptics Ltd., Cambridge, UK). Predominant DGGE bands were excised with a sterile filter tip, suspended in 50 µL of molecular biology grade water, and stored at 4 ºC overnight. The resuspended bands were subsequently reamplified by PCR as described above. Amplicons of the expected size were sequenced following Sanger's method at Macrogen (Macrogen, The Netherlands).

Sequences were processed using the BioEdit software package v.7.0.9 (Ibis Biosciences, Carlsbad, CA, USA) and aligned with the BLAST basic local alignment search tool (NCBI, Bethesda, MD, USA) and the Naïve Bayesian Classifier tool of RDP (Ribosomal Database Project) v.10 (East Lansing, MI, USA) for the taxonomic assignment.

Changes on the microbial community structure were analysed by covariance-based Principal Component Analysis (PCA) based on the position and relative intensity of the bands present on the DGGE profiles previously digitised. The MS Excel application StatistiXL v.1.4 (Broadway, Nedlands, Australia) was used for this purpose.

2.6.2 Quantitative PCR assay (qPCR)

The gene abundance of nitrifying, denitrifying and total eubacteria community was determined using quantitative PCR (qPCR). The qPCR amplification was performed for the

functional genes: ammonium monooxigenase (pair of primers *amoA*F/*amoA*R), which catalyzes the oxidation from ammonium to nitrite, and secondly the nitrous oxide reductase gene (pair of primers *nosZ*F/*nosZ*R [17]), which catalyzes the last step of the denitrification pathway from nitrous oxide to nitrogen gas. For the entire eubacteria community the *16S rRNA* gene was tested. Each sample was analyzed in triplicate by means of three independent DNA extracts. All reactions were performed using Brilliant II SYBR Green qPCR Master Mix (Stratagene, La Jolla, CA, USA) in a Real-Time PCR System Mx3000P (Stratagene) operated with the following protocol: 10 min at 95 °C, followed by 40 cycles of denaturation at 95 °C for 30 s, annealing for 30 s at 50 ºC, 54 ºC and 56 ºC (for *16S rRNA*, *amoA* and *nosZ* gene, respectively), extension at 72 °C for 45 s, and fluorescence capture at 80 °C (Table 2). The specificity of PCR amplification was determined by observations on a melting curve and gel electrophoresis profile. A melting curve analysis to detect the presence of primer dimers was performed after the final extension increasing the temperature from 55 to 95 °C at heating rates of 0.5 °C every 10 s. Image capture was performed at 82 °C to exclude fluorescence from the amplification of primer dimers. In all cases, the PCR reactions were performed in a total volume of 25 µL containing: 2 µL of DNA template, 200 nM of each *16S rRNA* primer, 600 nM of each primer, 12.5 µL of the ready reaction mix, and 30 nM of ROX reference dye. The primer set for *16S rRNA* and functional genes (*amoA* and *nos*Z) is described in Table 2. The standard curves were performed with the following reference genes: *16S rRNA* gene from *Desulfovibrio vulgaris* ATCC 29579 and *nosZ* gene from *Pseudomonas fluorescens* DSM 50415 as previously described [18] and a custom-made *amoA* synthetic gBlock™ gene fragment (IDT, IA, Coralville, USA) from Nitrosomonas europaea ATCC 19718, and a set of amoAF/amoAR primers [19].

All reference genes were quantified by NanoDrop 1000 (Thermo Scientific). Serial dilutions from 10^2 to 10^9 copies/reactions of plasmids/GBlocks™ containing known sequences of the

targeted genes in duplicate were used to generate the standard curves. The qPCR efficiencies of amplification for the *16S rRNA*, *nosZ*, and *amoA* genes were 108%, 83.1%, and 110.7% respectively. All results were processed with the MxPro qPCR Software (Stratagene).

2.6.3 Pyrosequencing and data analysis

The same DNA extracted from anode and cathode compartments and used for DGGE and qPCR analysis was used for pyrosequencing purposes. Each DNA sample was amplified separately using fusion primers containing adapters-barcode-forward primers (5'-3' direction) and a bead adapter-reverse primer (5'-3' direction). Reverse primers were bound to the beads by means of a specific bead adapter. Each sample was amplified with the *16S rRNA* eubacteria gene. The primer set for the eubacterial analysis population is described in Table 2. For the amplification 2µl of each DNA were used and the reaction was carried out in 50 µl containing 0.4 mM of fusion primers, 0.1 mM of dNTPs, 2.5 U of Taq ADN polymerase (Qiagen), and 5 µl of a reaction buffer (Qiagen). The PCR amplification operated with the following protocol: 30 s at 95 °C, followed by 30 cycles at 94 °C for 30 s, annealing at 55 °C for 30 s, and extension at 72 °C for 10 min. The PCR was carried out in a GeneAmp_PCRsystem 9700 termocicler (Applied Biosystems). Massive eubacterial *16S rRNA* gene libraries targeting the V3-V5 region were sequenced using the 454 FLX Titanium equipment developed by Roche Diagnostics (Branford, CT, USA). All PCR products obtained from the different samples using fusion primers were mixed in equal concentrations with the Quant-iT PicoGreen dsDNA Kit (Invitrogen, Carlsbad, CA, USA). Purification was achieved with Agencourt Ampure beads (Agencourt Bioscience Corporation, MA, USA). All sequencing protocols and reagents were executed as detailed by the manufacturer's guidelines.

The DNA readings obtained were compiled in FASTq files for further bioinformatics processing. Trimming of *16S rRNA* bar-coded sequences into libraries was carried out using

QIIME software version 1.8.0. Quality filtering of the readings was performed at Q25, prior to the grouping into Operational Taxonomic Units (OTUs) at a 97% sequence homology cut-off. The following steps were performed using QIIME: Denoising, using a Denoiser [20]; reference sequences for each OTU (OTU picking) were obtained via the first method of UCLUST algorithm; sequence alignment using PyNAST, and Chimera detection using ChimeraSlayer. OTUs were then taxonomically classified using BLASTn against GreenGenes databases and compiled into each taxonomic level.

2.6.4 Nucleotide Sequence Accession Numbers

All sequences derived from DGGE results have been submitted to the GenBank database under accession numbers, and data from pyrosequencing datasets were submitted to the Sequence Read Archive (SRA) of the National Centre for Biotechnology Information (NCBI) under the study accession number SRP051329.

3. RESULTS AND DISCUSSION

3.1 Nitrogen dynamics in the continuous aerated cathode period

3.1.1 MFC operation and nitrogen dynamics

The MFC was operated under the conditions described in Table 1. The MFC was operated in a continuous mode and under a organic loading rate (OLR) of 9.5 g COD L^{-1} d^{-1}, and a nitrogen loading rate (NLR) of 4.2 g $N\text{-}NH_4^+$ L^{-1} d^{-1}. Such high ammonium concentration did not cause any negative effect on the anode biofilm and over the overall MFC performance, as it has been reported in previous studies [21]. Polarization data were performed in order to analyse the MFC performance over time and under these operational conditions. Fig. 1a) shows four polarization curves at different stages from 3.5 months till 22 months. These results suggest that a potential exoelectrogenic biofilms was developed over time and the

power density (P_{max}) and current density (I_{max}) were increasing with successive stages from 34.4 mW/m^3 at 3.5 months to 806.8 mW/m^3 at 22 months.

During aerated cathode period (P.1) (Fig. 1b) an average voltage (V) of 193.9 mV, with a current density (I) of 2.3 A m^{-3} and a power density of 459.7 mW m^{-3} were achieved, while removing 53.8-69.1% of COD. The maximum power density obtained in polarization curves was 767.2±0.1 mW m^{-3}.

Fig. 1b) shows the nitrogen dynamics in a MFC harbouring active biomass both in the anode and cathode chambers. The results show that a range between 25.8±2.6% and 33.8±0.6% of total N-NH_4^+ migrated through the cation exchange membrane and, in the cathode, the diffused nitrogen found was: N-NH_4^+ (9.0±1.1% - 14.4±0.8%), N-NO_3^- (10.8±0.1% - 20.9±0.6%) and N-NO_2^- (<0.11%), with respect to the nitrogen transferred, resulting in nitrogen losses (notwithstanding the nitrites) ranging between (3.7±1.5% and 8.±0.2%). This indicates that the ammonium diffused though the membrane is being mostly nitrified at the cathode compartment. Although the optimum pH for nitrifying processes ranges from 8 to 9 [22], such process occurs as the main event in the cathode chamber with an average pH of 6.8±0.01 over time. Our results concur with those reported by Zhang and He [23], where the pH of the aerobic cathode was 6.7±0.2. These results were not as high as those for the MFCs reported by others [24] probably due to nitrification, which reduces alkalinity.

3.1.2 Microbial community assessment

In order to gain insight on the microbial community structure and its potential function related with the MFC operation, molecular biology methods such as DGGE and qPCR were applied to biomass from both the anode and the cathode chambers. As expected, DGGE results show a higher microbial diversity on the anode than in cathode chamber (Fig. 2). The predominant bands in the biofilm attached to the graphite granules of the anode chamber belonged to *Firmicutes*, *Bacteroidetes* and *Proteobacteria*. The most abundant classes within

the *Proteobacteria* phylum, have been *β-Proteobacteria*, as already reported in previous studies [25,26]. Park et al. [27] reported that *β-Proteobacteria* appears as the main population, rather than *α-Proteobacteria, γ-Proteobacteria* and *Flavobacteria*. The FISH analysis also shows that *β-Proteobacteria* was dominant on the biofilm-electrode, being *α-Proteobacteria* and *γ-Proteobacteria* rarely detected. They concluded that *β-Proteobacteria* was likely to play a key role in biofilm reactors.

The DGGE results from cathode chamber reveal *Nitrosomonas* sp. as the most predominant band which could highly contribute to nitrification process as an ammonium oxidizer (band 1 in Fig. 2a). Although *Nitrosomonas* sp. was identified as the main nitrifying bacteria linked to the nitration process, an important phylotype belonging to *Comamonadaceae* (band 2 in Fig. 2a) –a well-known potential denitrifier family–, was also present in the aerated cathode.

Regarding qPCR analyses, the *16S rRNA* gene copy number revealed a high abundance of total eubacterial populations both in the anode and cathode chamber (1.1×10^9 gene copy number g^{-1} and 6.2×10^8 gene copy number mL^{-1}, respectively). We also observed in the aerated cathode a high abundance of the *amoA* gene (8.9×10^9 gene copy number mL^{-1}), and even the presence of *nosZ* although at much lower concentrations (3.3×10^7 gene copy number mL^{-1}) (Fig. 2b). The high abundance of *amoA* gene at the cathode compartment explains the nitrification of the migrated ammonium. Furthermore, the presence of a *nosZ* gene suggests the possibility that a denitrification occurs under an optimal conditions at the cathode compartment, which agrees with the results obtained by DGGE.

To bear out the DGGE results from cathode chamber and analyse the cathodic microbial community in more detail, a 454-pyrosequencing was carried out on the cathode compartment. The results obtained revealed that the microbial community was mainly accounted for with three phyla, *Proteobacteria* (71.9%), *Bacteroidetes* (26.4%) and *Actinobacteria* (1.5%) in a minor degree. Looking at the family level, *Nitrosomonadaceae*

(44.5%) appears to be the most predominant family whereas an important community belonging to *Comamonadaceae* (21.4%) and *Chitinophagaceae* (11.9%) is also concomitant to the nitrifying community of the cathode chamber (Fig. 3a), as also observed in the DGGE results (Fig. 2a).

Pyrosequencing data also revealed class *β-Proteobacteria* as the dominant group of bacteria accounting for 66.4%, followed by *Flavobacteria* with 14.5%, and *Sphingobacteria* with 11.9% of the relative abundance on reads obtained from the cathode chamber, as previously described by [26]. The group of *α-Proteobacteria* scarcely appeared with only 4.7% of the sequences and *γ-Proteobacteria* were not identified at all. These results are in excellent agreement with Cong et al. [28] who found a pronounced enrichment in *β-Proteobacteria* and *Sphingobacteria* attached to the biofilm-electrode and demonstrated that bacteria consortiums with current acclimation had higher levels of β- than α-*Proteobacteria*. Moreover, *Sphingobacteria* were identified to be dominant in denitrifying cathode biofilms. In our study, the β-proteobacteria class was mainly comprised by *Nitrosomonas* sp. (44.5%), and *Comamonas* sp. (19.9%), whereas the Flavobacteria class included *Kaistella* sp. (10.8%).

These results point out to the possibility of enhancing denitrification by promoting sequential aerobic-anoxic conditions in the cathode. Nevertheless, as a first step, and in order to confirm the presence of a denitrifying microbial community, the cathodic biomass was grown in a set of different denitrification batch assays.

3.2 Denitrification batch assays

Batch experiments were carried out in anoxic conditions to confirm the occurrence of denitrification processes on biomass harvested from cathode chamber. Denitrification occurred when acetate was added to the cathode effluent, reaching up to 99.7% (from 128.9 to 0.4 mg $N\text{-}NO_3^-$ L^{-1}) of the nitrate removal in 7 days. However, nitrate removal was quite low, reaching just 16.5% (from 64.5 to 53.8 mg $N\text{-}NO_3^-$ L^{-1}) when an anode effluent was

combined with the cathode effluent (without acetate amendment but containing the non-degraded acetate), and only 5.1% (from 128.9 to 122.4 mg $N\text{-}NO_3^-$ L^{-1}) of nitrate removal was accomplished using just the cathode effluent without additional acetate in these batch experiments (Fig. 4). These results suggest that there is no autotrophic denitrification under these conditions; however, the existence of a heterotrophic denitrification is confirmed by the microbial community analysis (Fig. 4 and 5a).

3.2.1 Microbial community assessment

Comparison between the physicochemical analysis and the DGGE results revealed the presence of well known denitrifying phylotypes, when acetate was added to cathode effluent. The three predominant bands (bands 5, 6 and 7) (Fig. 5a) belonged to *Burkholderiaceae*, *Alcaligenaceae* and *Comamonadaceae*, (Table 3), which have been previously reported as key players in cathodic nitrate reduction in a closed circuit [13].

In the other batch conditions, without acetate amendment, minority bands (bands 4 and 11) like *Comamonadacea* and *Alcaligenaceae,* (Table 3) were identified as potential denitrifiers.

The rest of the bands identified on the DGGE belong mostly to *Bacteroidetes* (*Porphyromonadaceae*) and *Proteobacteria* (β and γ-*Proteobacteria*), which have been also described as dominant phyla in other MFCs systems [26,29].

The Multivariate Principal Component Analysis (PCA) of the DGGE profiles (Fig. 5b) showed three distinct main groups. One group corresponds to the samples from the cathode chamber and the batch experiments with cathode effluent without acetate addition. Although nitrate was not consumed during the denitrification batch experiment performed with only the cathode effluent, some bands showing phylotypes potentially related with denitrification processes were described. It is worth noting that acetate addition into the cathode effluent caused a significant shift on the DGGE profile, with the occurrence of potential denitrifying phylotypes as well as the enhancement of the denitrification process. DGGE profile

differentiation of the cathode effluent + the acetate and cathode effluent + the anode effluent batch experiments, displayed as separate groups on the PCA, might be explained by the different microbial communities encompassed in both compartments, as well as by the difference in acetate availability, being residual in the anode effluent and clearly higher when acetate was added directly to the batch experiment (COD of 1.120 mg O_2 L^{-1}).

Therefore, denitrification batch assays confirm the existence of a potential denitrifying population in the cathode chamber which could be enhanced if the cathode is adequately operated.

3.3 Nitrogen dynamics during the intermittent aerated cathode periods

3.3.1 MFC operation and nitrogen dynamics

Since the previous experiments indicated that a potential denitrifying community was concomitant with the nitrifying population, the cathode compartment was submitted to different working conditions in order to achieve simultaneous nitrification-denitrification processes. The oxidation of ammonium to nitrate, conducted as shown mainly by *Nitrosomonas* sp., in the continuous aerated cathode (P.1) was one of the main processes taking place and, as a result, a high accumulation of nitrate was detected in the cathode chamber (169.4±0.21 mg $N\text{-}NO_3^-$ L^{-1}). These results, and the finding of a potential denitrifying community, suggested that establishing nitrification-denitrification processes may be feasible if the cathode is submitted to aerobic-anoxic cycles.

In order to evaluate whether the intermittent aerated periods had an influence on the cathode denitrifying community and its ability to reduce nitrate, the evolution of nitrogen ($N\text{-}NH_4^+$, $N\text{-}NO_3^-$ and $N\text{-}NO_2^-$) both in the anode and in the cathode compartments was studied. The initial nitrate concentration in the cathode was 169.4±0.21 mg $N\text{-}NO_3^-$ L^{-1}, which was higher than other concentrations from previous studies on autotrophic nitrate reduction such as 26 and 50 mg $N\text{-}NO_3^-$ L^{-1} [12,30], though two-fold lower than the experimental conditions

described by Park et al. [27]. Fig. 6a) shows the evolution of the different forms of nitrogen during three short intermittent aerated cycles (P. 2.1). As it can be seen, ammonia concentrations decreased during the aerated periods whereas nitrates decreased during the non-aerated periods. In Table 4 we can see that the reported average $N\text{-}NO_3^-$ removal efficiency was 17.8% (P. 2.1). The same behaviour, though with a lower $N\text{-}NO_3^-$ 8.3% removal efficiency, was also observed during the long intermittent aerated period (P. 2.2). Nevertheless, when acetate was added (P. 2.3) the removal efficiency increased up to 41.2% (Fig. 6b).

As nitrate reduction to di-nitrogen gas occurs through four consecutive reactions where two of them tend to accumulate (NO_2^- and N_2O) [31], nitrite concentrations were as well monitored. During the two first non-aerated cycles of the intermittent aerated period (P. 2.1) the accumulation of nitrite was 4.3 and 10.9 mg $N\text{-}NO_2^- L^{-1}$, respectively (Fig. 6b), although this concentration reached 0 during the second non-aerated period (P. 2.2). The decrease in nitrite accumulation after some non-aerated cycles could be due to an acclimation of the denitrification processes. Pous et al. [32] reported concentrations close to 0 after 84 days. Nevertheless it is surprising that in the last non-aerated period, when the acetate was added, nitrite concentrations rose to higher values than in previous periods, reaching up to 15.8 mg $N\text{-}NO_2^- L^{-1}$.

The pH of the catholyte showed a slightly increased during the intermittent aerated periods, from 6.41 to 6.45; 6.45 to 6.53, and 6.44 to 6.55 for the three non-aerated periods shown in Fig. 6a), and from 6.89 to 7.11; 6.49 to 6.61; 6.81 to 6.97; 6.94 to 6.99, and 6.70 to 6.74 for the five non-aerated periods shown in Fig. 6b). Although the optimum pH for denitrification processes is between 7 and 8 [33], these values, lower than 7, do not seem to affect the presence of potential nitrous oxide reductase genes to catalyse the last step of the denitrification pathway taking place with a pH value below 6 [34].

Although residual nitrogen was still present, the use of MFC to partially remove nitrogen could be a good strategy to adjust the composition of either high strength wastewater or livestock wastewater, to be used as fertilizer.

3.3.2 Microbial community assessment

The microbial community was quantified by means of qPCR and pyrosequencing, both in the aerated cathode and in the last stage of each intermittent aerated period. The results showed that the abundance of the *16S rRNA* gene varied between $5.9x10^{9}$ gene copy number mL^{-1} on the aerated cathode (P. 1) and a range between $3.1x10^{10}$- $4.7x10^{10}$ gene copy number mL^{-1} on the intermittent aerated cathode periods (P. 2.1, 2.2 and 2.3) (Fig. 7). The amount of *16S rRNA* genes increased slightly during the intermittent aerated periods. Likewise, the *amoA* gene increased during the intermittent aerated cathode periods (P. 2.1, 2.2 and 2.3), compared with the continuous aerated cathode period (P. 1) ranging from $8.9x10^{9}$ to $3.1x10^{10}$ gene copy number mL^{-1}. Regarding the *nos*Z gene, linked to denitrification, its gene copy number experienced a 3-7 fold increase, from $3.3x10^{7}$ gene copy number mL^{-1} on the continuous aerated cathode period (P. 1) to $9.6x10^{7}$-$1.6x10^{8}$ on the intermittent aerated cathode periods (P. 2.1 an 2.2); and to $2.4x10^{8}$ on the intermittent aerated cathode period with the addition of acetate (P. 2.3) (Fig. 7). Besides, the gene ratio *nos*Z/*16S rRNA* shifted from 0.08 to 0.15 after the intermittent aerated periods, which speaks of an enrichment of denitrifying populations when aeration is stopped and the cathode chamber is fed with acetate as a carbon source and an alternative electron donor.

As for the pyrosequencing analysis, although the Phyla *Proteobacteria, Bacteroidetes* and *Actinobacteria* are still dominant, a clear shift at lower taxonomic levels is noticed during different operational conditions. Under intermittent aerated periods new denitrifying families such as *Phyllobacteriaceae* (1.0%), *Xanthomonadaceae* (8.2%), *Sphingomonadaceae* (1.1%), and *Oxalobacteriaceae* (1.1%) were also enriched (Fig. 3b). When acetate was added to the

intermittent aerated period this denitrifying community was clearly enriched in *Comamonadaceae* phylotypes, increasing from 19.5% to 35.4% (Fig. 3c). Regarding the nitrifying community, its diversity and structure was quite stable and represented by a high relative abundance of *Nitrosomonas* sp. (as AOB) (44.5%, 23.0% and 27.2% in P. 1, 2.2 and 2.3 respectively) and *Nitrobacter* sp. (as nitrite oxidizer, NOB) (1.0%, 10.9% and 5.1% in P. 1, 2.2 and 2.3 respectively); also in samples from the intermittent aerated cathode periods. The diversity indexes –the inverted Simpson index and Shannon-Wiever index–, confirm that the overall diversity of the samples remained stable over the different periods, with values of 21.5 (P. 1), 32.2 (P. 2.2) and 24.9 (P. 2.3) for the inverted Simpson index, and 3.9 (P. 1), 3.9 (P. 2.2) and 3.8 (P. 2.3) for the Shannon-Wiever index.

Summing up, while the nitrifying community abundance remains stable in quantity and diversity throughout time, regardless of the working conditions, the denitrifying community increases under the application of intermittent aeration periods. Further research is needed to ascertain the real denitrification mechanisms (either heterotrophic or mixotrophic) that have been occurring in the cathode in the presence of low concentration of organic compounds and electron donors, which compete with the electrons coming from the circuit.

4. CONCLUSIONS

The nitrification of the diffused ammonia (30.4%) was the main process happening at the aerated cathode and denitrification processes could be enhanced to reach a nitrate removal efficiency of 41.2%, when intermittent aeration cycles plus acetate were applied.

Additionally, microbiology analysis showed that the microbial community structure was dominated by concomitant nitrifying (*Nitrosomonas* sp.) and denitrifying members (*Alcaligenaceae, Burkholderiaceae* and *Comamonadaceae*). Moreover, when intermittent aerated periods were applied, mixotrophic-driven denitrification could be the main mechanism for denitrification at the cathode compartment under these conditions, thus

confirming the feasibility of nitrification-denitrification processes in the cathode when intermittent aeration is applied.

Acknowledgements

This research was funded by the Spanish Ministry of Science and Innovation (MICINN project CTM2009-12632 and INIA project RTA2012-00096-00-00). The authors wish to thank Joan Noguerol and Eva Romero for their support on physicochemical analysis and Miriam Guivernau and Arantxa Matos for their support in microbiology aspects.

References

[1] S.A.R. Mousavi, S. Ibrahim, M.K. Aroua, S. Ghafari, Bio-electochemical denitrification-A review, Intern. J. Chem. Environ. Engin. 2 (2011).

[2] F. Zhang, Z. He, A cooperative microbial fuel cell system for waste treatment and energy recovery, Environ. Technol. 34 (2013) 1905-1913.

[3] B. Logan, B. Hamelers, R. Rozendal, U. Schröder, J. Keller, S. Freguia, P. Aelterman, W. Verstraete, K. Rabaey, Microbial fuel cells: methodology and technology, Environ. Sci. Technol. 40 (2006) 5181-5192.

[4] K. Rabaey, J. Rodriguez, L.L. Blackall, J. Keller, P. Gross, D.J. Batstone, Microbial ecology meets electrochemistry: electricity-driven and driving communities, ISME J. 1 (2007) 9-18.

[5] B. Min, J. Kim, S. Oh, J.M. Regan, B.E. Logan, Electricity generation from swine wastewater using microbial fuel cells, Water Res. 39 (2005) 4961-4968.

[6] R.A. Rozendal, T. Sleutels, H.V.M. Hamelers, C.J.N. Buisman, Effect of the type of ion exchange membrane on performance, ion transport, and pH in biocatalyzed electrolysis of wastewater, Water Sci. Tecnol. 57 (2008) 1757-1762.

[7] J. Desloover, A.A. Woldeyohannis, W. Vestraete, N. Boon, K. Rabaey, Electrochemical resource recovery from digestate to prevent ammonia toxicity during anaerobic digestion, Environ. Sci. Technol. 46 (2012) 12209-12216.

[8] P. Clauwaert, K. Rabaey, P. Aelterman, L. DeSchamphelaire, T.H. Pham, P. Boeckx, N. Boon, W. Verstraete, Biological denitrification in microbial fuel cells, Environ. Sci. Technol. 41 (2007) 3354-3360.

[9] B. Virdis, K. Rabaey, Z. Yuan, J. Keller, Microbial fuel cells for simultaneous carbon and nitrogen removal, Water Res. 42 (2008) 3013-3024.

[10] B. Virdis, S.T. Read, K. Rabaey, R.A. Rozendal, Z. Yuan, J. Keller, Biofilm stratification during simultaneous nitrification and denitrification (SND) at a biocathode, Bioresor. Technol. 102 (2010) 334-341.

[11] W.G. Zumft, Cell biology and molecular basis of denitrification, Microbial Mol. Biol. Rev. 61 (1997) 533-616.

[12] A. Vilar-Sanz, S. Puig, A. García-Lledó, R. Trias, M.D. Balaguer, J. Colprim, Ll. Bañeras, Denitrifying bacterial community affect current production and nitrous oxide accumulation in a microbial fuel cell, PLoS One. 8 (2013), e63460.

[13] K.C. Wrighton, B. Virdis, P. Clauwaert, S.T. Read, R.A. Daly, N. Boon, Y. Piceno, K.C. Arighton, B. Virdis, P. Clauwaert, S.T. Read, R.A. Daly, N. Boon, Y. Piceno, G.L. Andersen, J.D. Coates, K. Rabaey, Bacterial community structure corresponds to performance during cathodic nitrate reduction, ISME J. 4 (2010) 1443-1455.

[14] H. Lu, A. Oehmen, B. Virdis, J. Keller, Z. Yuan, Obtaining highly enriched cultures of *Candidatus Accumulibacter* phosphates through alterating a carbon sources, Water Res. 40 (2006) 3838-3848.

[15] APHA, AWA, WEF., Standard methods for the examination of water and waste water, 21th ed. American Public Health Association/American Water Works Association/Water Environment Federation, Washington, DC, USA. (2005)

[16] Z. Yu, M. Morrison, Comparisons of different hypervariable regions of *rrs* genes for use in fingerprinting of microbial communities by PCR-denaturing gradient gel electrophoresis, Appl. Environ. Microbiol. 70 (2004) 4800-4806.

[17] E. Kandeler, K. Deiglmayr, D. Tscherko, D. Bru, L. Philippot, Abundance of narG, nirS, nirK, and nosZ genes of denitrifying bacteria during primary successions of a glacier foreland, Appl. Environ. Microbiol. 72 (2006) 5957-5962.

[18] M. Calderer, V. Martí, J. De Pablo, M. Guivernau, F.X. Prenafeta-Boldú, M. Viñas, Effects of enhanced denitrification on hydrodynamics and microbial community structure in a soil column system, Chemosphere 111 (2014) 112-119.

[19] Y. Shimomura, S. Morimoto, Y. Takada Hoshino, Y. Uchida, H. Akiyama, M. Hayatsu, Comparison among amoA primers suited for quantification and diversity analyses of ammonia-oxidizing bacteria in soil, Microbes Environ. 27 (2012) 94-98.

[20] J. Reeder, R. Knight, Rapidly denoising pyrosequencing amplicon reads by exploiting rank-abundance distributions, Nat. Methods. 7 (2010) 668-669.

[21] A. Sotres, M. Cerillo, M. Viñas, A. Bonmatí, Nitrogen recovery from pig slurry in a two-chambered bioelectrochemical system, Bioresour. Technol. 194 (2015) 373-382.

[22] R.C. Anthonisen, R.C. Loehr, T.B.S. Prakam, E.G. Srinath, Inhibition of nitrification by ammonia and nitrous acid, Water Environm. Federation. 48 (1976) 835-852.

[23] F. Zhang, Z. He, Simultaneous nitrification and denitrification with electricity generation in dual-cathode microbial fuel cells, J. Chem. Technol. Biotechnol. 87 (2011) 153-159.

[24] F. Zhao, F. Hamisch, U. Schroder, F. Scholz, P. Bogdanoff, I. Hermann, Challenges and constrains of using oxygen cathodes in microbial fuel cells, Environ. Sci. Technol. 40 (2006) 5193-5199.

[25] A. Bonmatí, A. Sotres, Y. Mu, R. Rozendal, K. Rabaey, Oxalate degradation in a bioelectrochemical system: reactor performance and microbial community characterization, Bioresour. Technol. 143 (2013) 147-153.

[26] A. Sotres, J. Diaz-Marcos, M. Guivernau, J. Illa, A. Magrí, F.X. Prenafeta-Boldú, A. Bonmati, M. Viñas, Microbial community dynamics in two-chambered microbial fuel cells: Effect of different ion exchange membranes, J. Chem. Technol. Biotechnol. (2014) DOI:10.1002/jctb.4465.

[27] Ho II Park, J.S. Kim, D.K. Kim, Y-J. Choi, D. Pak, Nitrate-reduncing bacterial community in a biofilm-electrode reactor, Enzyme Microb. Technol. 39 (2006) 453-458.29.

[28] Y. Cong, Q. Xu, H. Feng, D. Shen, Efficient electrochemically active biofilm denitrification and bacteria consortium analysis, Bioresour. Technol. 132 (2013) 24-27.

[29] J. Huang, Z. Wang, Ch. Zhu, J. Ma, X. Zhang, Z. Wu, Identification of microbial communities in open and closed circuit bioelectrochemical MBRs by High-throughput 454 pyrosequencing, PLoS One. 9 (2014) e93842.

[30] K.C. Lee, B.E. Rittman, Applying a novel autohydrogenoiotrophic hollowfiber membrane biofilm recator for denitrification of drinking water, Water Res. 36 (2002) 2040-2052.

[31] B. Virdis, K. Rabaey, Z. Yuan, R.A. Rozendal, J. Keller, Electron fluxes in a microbial fuel cell performing crabon and nitrogen removal, Environ. Sci. Technol. 43 (2009), 5144-5149.

[32] N. Pous, S. Puig, M.D. Balaguer, J. Colprim, Cathode potential and anode electron donor evaluation for a suitable treatment of nitrate-contaminated groundwater in bioelectrochemical systems, Chem. Engin. J. 263 (2015) 151-159.

[33] Y.H. Ahn, Sustainable nitrogen elimination biotechnologies: A review, Process Biochem. 41 (2006) 1709-1721.

[34] O. Einsle, P.M.H. Kroneck, Structural basis of denitrification, Biol. Chem. 385 (2004), 875-883.

Table 1

Set up and operational characteristics of the anode and cathode chambers.

Methacrylate chamber (internal dimensions)	0.14 x 0.12 x 0.002 m^3
Net anodic volume (NAV)	165 mL
Net cathodic volume (NCV)	250 mL
HRT (A)	6.3 h
HRT (C)	9.4 h
Initial inoculum	Anaerobic biomass
Organic loading rate (OLR)	9.5 g COD L^{-1} d^{-1}
Nitrogen loading rate (NLR)	4.2 g N-NH_4^+ L^{-1} d^{-1}
Electrode (anode) Electrode (cathode)	Granular graphite Stainless steel mesh
External resistor	500 Ω
Cation exchange membrane	Ultrex CMI-7000

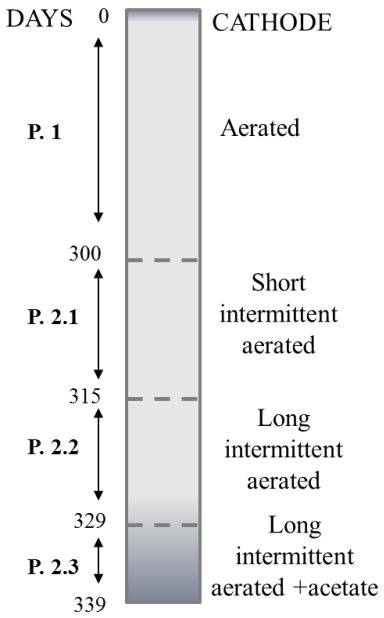

Table 2

Primers and conditions used for DGGE-PCR, qPCR and 454-pyrosequencing.

Gene	Primers	Sequence (5'-3')	PCR type	Conditions
16S rRNA	341F-GC[1]	CCTACGGGAGGCAGCAG	PCR-DGGE	Primer conc: 0.25µM
	907R	CCGTCAATTCCTTTRAGTTT		Anneling temp: 55º
16S rRNA	519F	GCCAGCAGCCGCGGTAAT	qPCR	Primer conc: 200nM
	907R	CCGTCAATTCCTTTGAGTT		Annealing: 50º
amoA	amoAF	GGGGTTTCTACTGGTGGT	qPCR	Primer conc: 200nM
	amoAR	CCCCTCKGSAAAGCCTTCTTC		Annealing: 54º
nosZ	nosZF	CGYTGTTCMTCGACAGCCAG	qPCR	Primer conc: 200nM
	nosZR	CAKRTGCAKSGCRTGGCAGAA		Annealing: 56º
16S rRNA	27Fmod	AGRGTTTGATCMTGGCTCAG	454-pyroseq	Primer conc: 0.4mM
	519RmodBio	GTNTTACNGCGGCKGCTG	454-pyroseq	Annealing: 55º

[1] GC clamp: 5'-CGCCCGCCGCGCCCCGCGCCCGTCCCGCCGCCCCCGCCCG-3'

Table 3

Characteristics of the bands excised and sequenced from Eubacterial *16S rRNA* gene based-DGGE (Fig. 5a) from samples obtained in denitrification batch experiments.

Band	Length (bp)	Accession number	Closet organism in GenBank database (accession number)	Similarity (%)	Phylogenetic group (RDP)
1	480	JQ307401	Uncultured Bacteroidetes bacterium (GU112204)	99%	*Bacteroidetes*
2	357	JQ307402	Uncultured bacterium (EF559196)	98%	*Bacteroidetes*
3	425	JQ307403	*Acinetobacter seohaensis* (FJ392126)	100%	*Moraxellaceae Gammaproteobacteria*
4	415	JQ307404	*Comamonas sp* (HM365952)	99%	*Comamonadaceae Betaproteobacteria*
5	361	JQ307405	*Comamonas sp* (FJ426595)		*Comamonadaceae Betaproteobacteria*
6	270	JQ307406	*Tetrathiobacter mimigardefordensis* (HM031463)	99%	*Alcaligenaceae Betaproteobacteria*
7	440	JQ307407	Uncultured Bacteroidetes bacterium (CU923099)	94%	*Porphyromonadaceae Bacteroidetes*
8	499	JQ307408	Uncultured bacterium (AM982611)	95%	*Bacteroidetes*
9	471	JQ307409	*Proteiniphilum acetatigenes* (AY742226)	97%	*Porphyromonadaceae Bacteroidetes*
10	432	JQ307410	*Bacteroides coprosuis* (AF319778)	99%	*Bacteroidaceae Bacteroidetes*
11	438	JQ307411	*Alcaligenes faecalis* (HM597239)	99%	*Alcaligenaceae Betaproteobacteria*
12	475	JQ307412	*Acholeplasma sp* (FN813713)	95%	*Acholeplasmataceae Mollicutes*

Table 4

Effect of the intermittent aerated periods on the nitrate removal efficiency at cathode chamber.

Period	$N\text{-}NH_4^+$ transferred	$\eta_{N\text{-}NO3^-}$
P. 2.1 (Short intermittent aerated cathode)	29.9±0.1 %	17.8±2.5 %
P. 2.2 (Long intermittent aerated cathode)	21.8±0.1 %	8.3±2.5 %
P. 2.3 (Long intermittent aerated cathode + acetate)	32.6±0.1 %	41.2±4.4 %

FIGURE CAPTIONS

Fig. 1. (a) Polarization curves at different stages, and (b) voltage and nitrogen evolution over time during period 1-continuous aeration cathode (data shows 3 samples periods).

Fig. 2. (a) Total eubacterial community DGGE profile in the anode biofilm-electrode and in the biomass located in the supernatant aerated cathode chamber. (b) *16S rRNA*, *nos*Z and *amo*A genes for both compartments.

Fig. 3. Taxonomic assignment of 16SrRNA based-pyrosequencing assessment of bacterial community at the aerated cathode chamber during the different periods: (a) continuous aerated cathode - period 1- (phylum (i), class (ii), order (iii) and family (iv) level); (b) intermittent aerated period – period 2.2 - (family level) ; and (c) during the intermittent aerated period + acetate - period 2.3- (family level). Note: Phylogenetic groups with relative abundance lower that 1% were categorized as "others".

Fig. 4. $N\text{-}NO_3^-$ removal in the denitrification batch assays using cathode effluent from MFC cathode chamber and different biomass sources after 7 days. In brackets, nitrate removal percentage.

Fig. 5. (a) DGGE 16SrDNA (V_3-V_5 region) of the total eubacteria microbial community from the different batch assays and (*) sample from MFC cathode chamber. (b) Principal Component Analysis (PCA) 2D-Plot from DGGE profiles. In brackets, the percentage of nitrate removal after 7d of incubation in the denitrification batch assays.

Fig. 6. Nitrogen dynamics ($N\text{-}NO_3^-$, $N\text{-}NO_2^-$ and $N\text{-}NH_4^+$) in the cathode during the intermittent aerated periods. (a) Short intermittent aerated cycles (period 2.1), and (b) Long intermittent aerated cycles with addition of acetate (period 2.3).

Fig. 7. Abundances of the *16S* rRNA and two functional genes (*amo*A and *nos*Z) according to the last point of four periods studied. The number of copies for these genes (a) functional genes (*amo*A and *nos*Z) and (b) *16S* rRNA and *nos*Z at aerated cathode, after two non-aerated cathode periods and non-aerated period with acetate pulses. Standard errors of the mean (n=3) are indicated.

Fig. 1

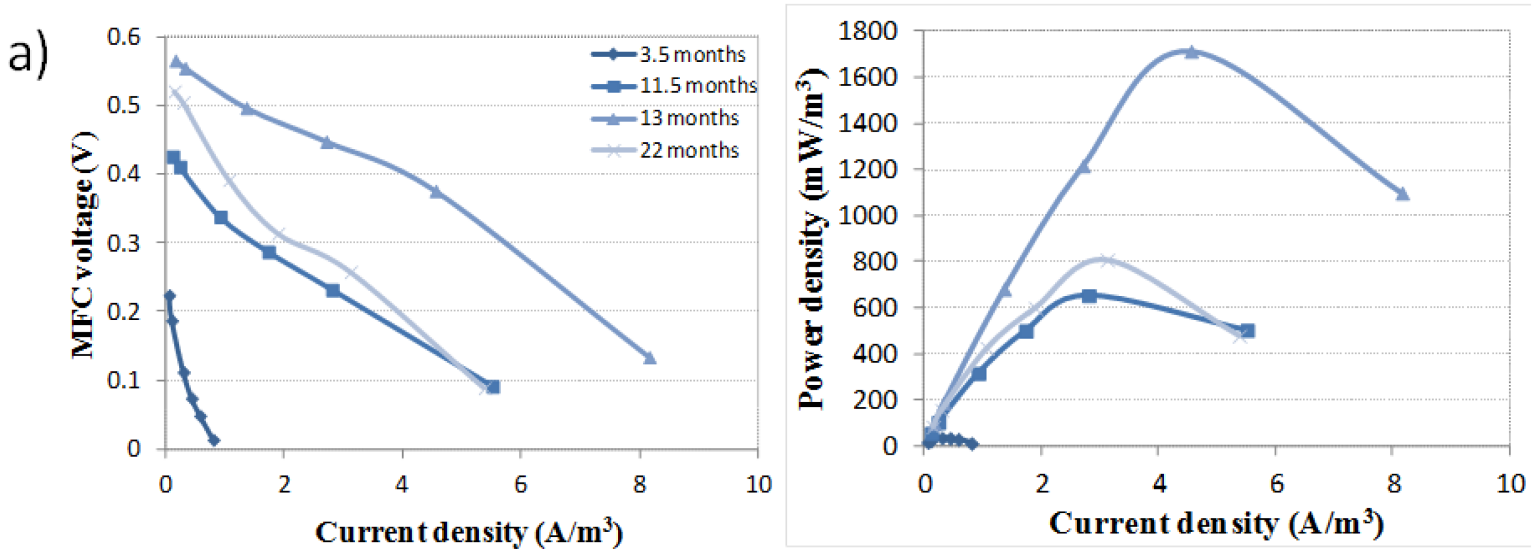
a)
MFC voltage (V)
Current density (A/m³)
3.5 months
11.5 months
13 months
22 months
Power density (mW/m³)
Current density (A/m³)

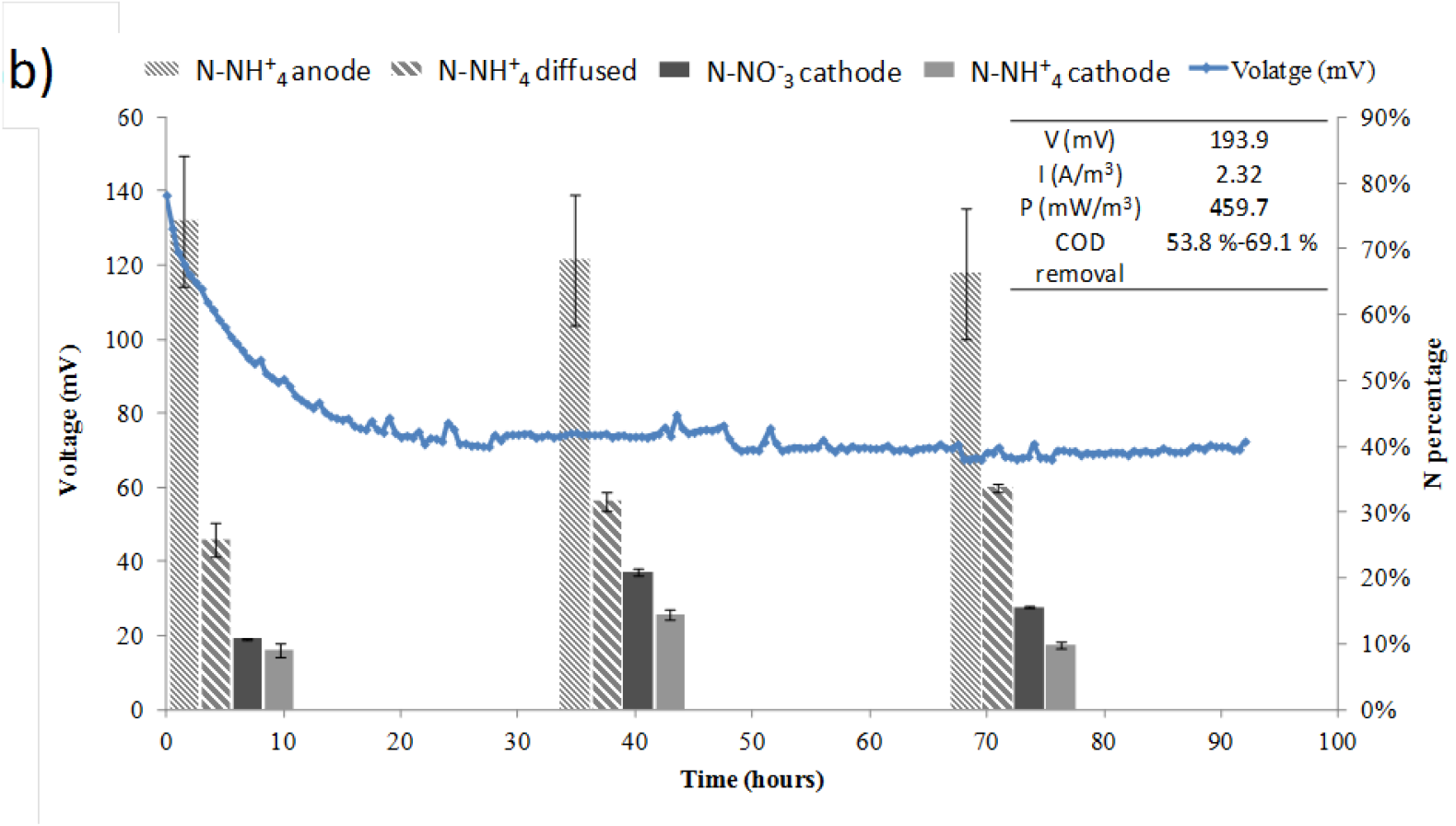
b)
N-NH⁺4 anode
N-NH⁺4 diffused
N-NO⁻3 cathode
N-NH⁺4 cathode
Volatge (mV)
V (mV) 193.9
I (A/m³) 2.32
P (mW/m³) 459.7
COD removal 53.8 %-69.1 %
Voltage (mV)
N percentage
Time (hours)

Fig. 2

a)

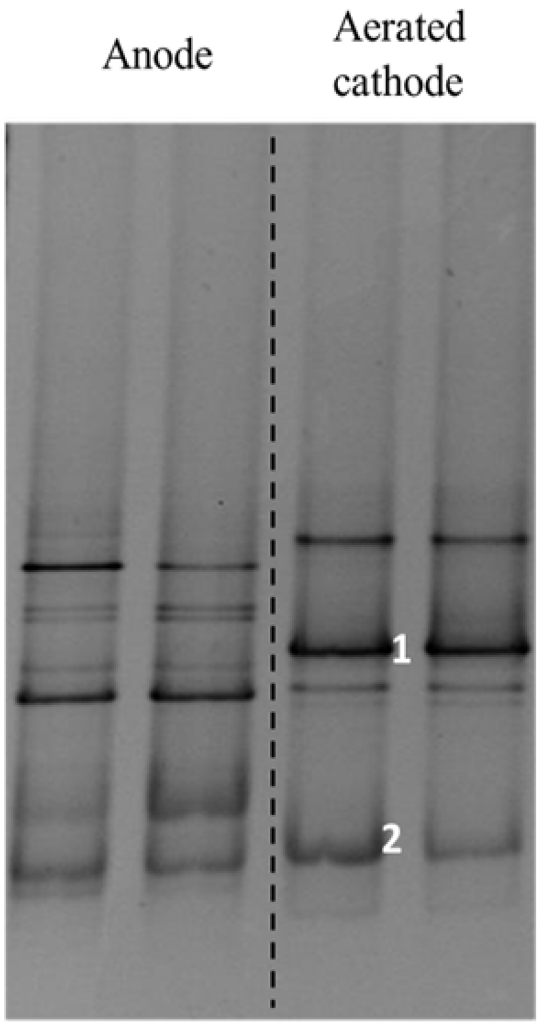

b)

Gene	Anode (gene copy number/g)	Aerated cathode (gene copy number/mL)
16S rRNA	$1.1\pm0.6\times10^{9}$	$6.2\pm0.5\times10^{8}$
nosZ	$3.1\pm0.6\times10^{9}$	$3.3\pm0.8\times10^{7}$
amoA	$2.4\pm1.4\times10^{4}$	$8.9\pm0.8\times10^{9}$

Fig. 3

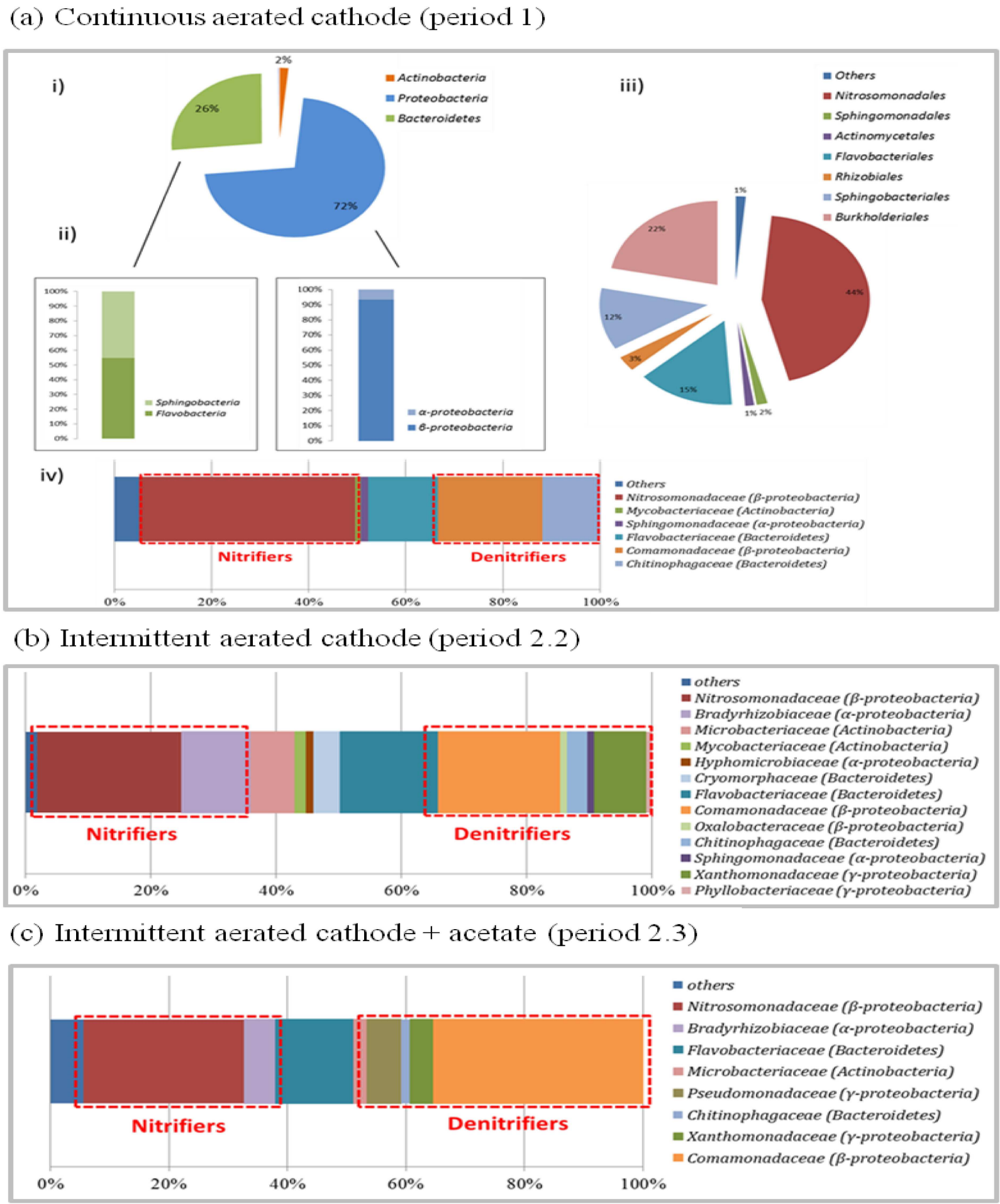
(a) Continuous aerated cathode (period 1)
i)
2%
26%
72%
Actinobacteria
Proteobacteria
Bacteroidetes
ii)
Sphingobacteria
Flavobacteria
α-proteobacteria
δ-proteobacteria
iii)
Others
Nitrosomonadales
Sphingomonadales
Actinomycetales
Flavobacteriales
Rhizobiales
Sphingobacteriales
Burkholderiales
1%
22%
44%
12%
3%
15%
1% 2%
iv)
Nitrifiers
Denitrifiers
Others
Nitrosomonadaceae (β-proteobacteria)
Mycobacteriaceae (Actinobacteria)
Sphingomonadaceae (α-proteobacteria)
Flavobacteriaceae (Bacteroidetes)
Comamonadaceae (β-proteobacteria)
Chitinophagaceae (Bacteroidetes)
0%
20%
40%
60%
80%
100%
(b) Intermittent aerated cathode (period 2.2)
Nitrifiers
Denitrifiers
others
Nitrosomonadaceae (β-proteobacteria)
Bradyrhizobiaceae (α-proteobacteria)
Microbacteriaceae (Actinobacteria)
Mycobacteriaceae (Actinobacteria)
Hyphomicrobiaceae (α-proteobacteria)
Cryomorphaceae (Bacteroidetes)
Flavobacteriaceae (Bacteroidetes)
Comamonadaceae (β-proteobacteria)
Oxalobacteraceae (β-proteobacteria)
Chitinophagaceae (Bacteroidetes)
Sphingomonadaceae (α-proteobacteria)
Xanthomonadaceae (γ-proteobacteria)
Phyllobacteriaceae (γ-proteobacteria)
0%
20%
40%
60%
80%
100%
(c) Intermittent aerated cathode + acetate (period 2.3)
Nitrifiers
Denitrifiers
others
Nitrosomonadaceae (β-proteobacteria)
Bradyrhizobiaceae (α-proteobacteria)
Flavobacteriaceae (Bacteroidetes)
Microbacteriaceae (Actinobacteria)
Pseudomonadaceae (γ-proteobacteria)
Chitinophagaceae (Bacteroidetes)
Xanthomonadaceae (γ-proteobacteria)
Comamonadaceae (β-proteobacteria)
0%
20%
40%
60%
80%
100%

Fig. 4

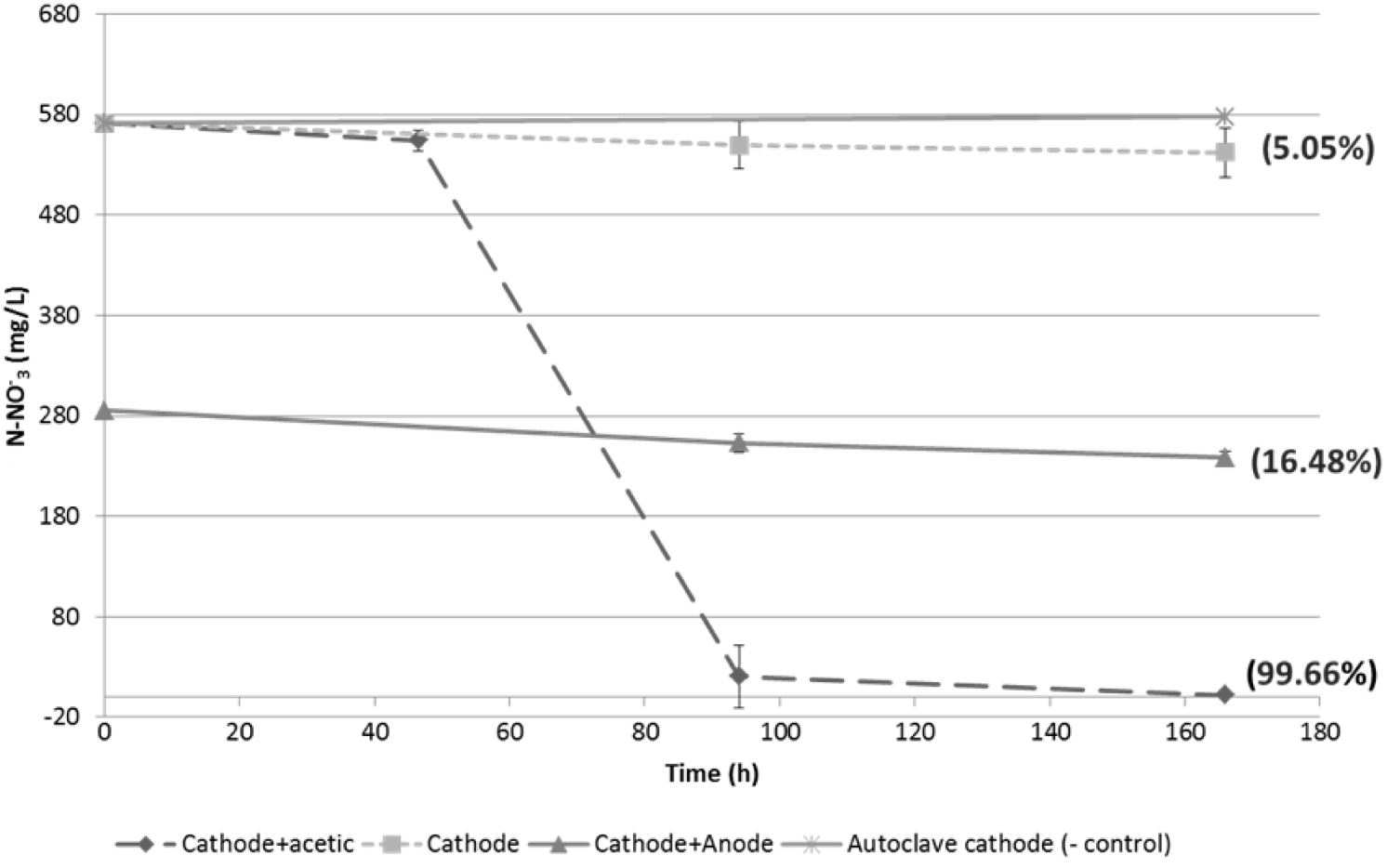
680
580
480
380
280
180
80
-20
N-NO3 (mg/L)
0
20
40
60
80
100
120
140
160
180
Time (h)
(5.05%)
(16.48%)
(99.66%)
Cathode+acetic
Cathode
Cathode+Anode
Autoclave cathode (- control)

Fig. 5

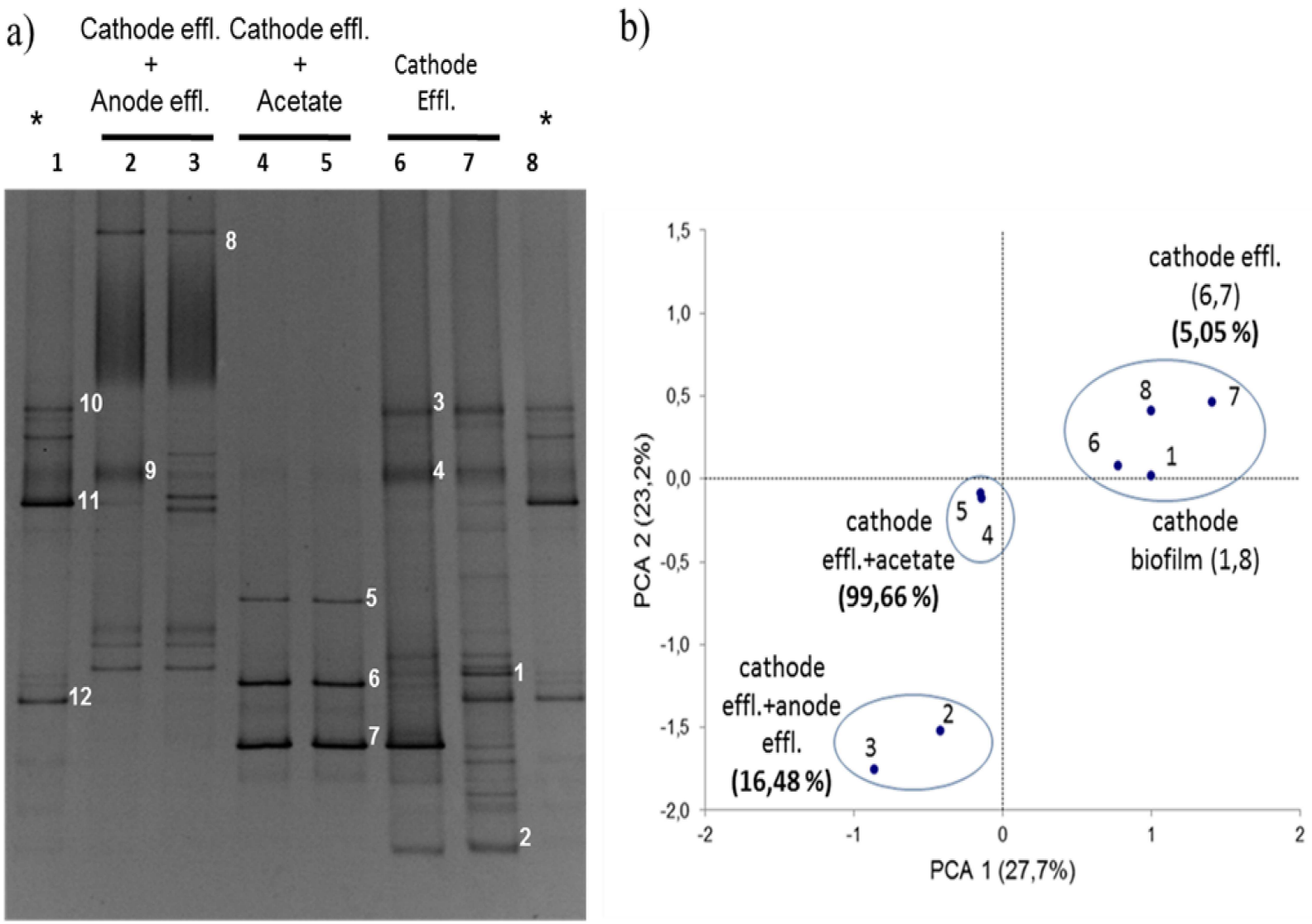
a)
Cathode effl. + Anode effl.
Cathode effl. + Acetate
Cathode Effl.
*
1
2
3
4
5
6
7
8
*
10
11
12
9
8
5
6
7
3
4
1
2
b)
cathode effl. (6,7) (5,05 %)
cathode effl.+acetate (99,66 %)
cathode biofilm (1,8)
cathode effl.+anode effl. (16,48 %)
PCA 1 (27,7%)
PCA 2 (23,2%)
1,5
1,0
0,5
0,0
-0,5
-1,0
-1,5
-2,0
-2
-1
0
1
2

Fig. 6

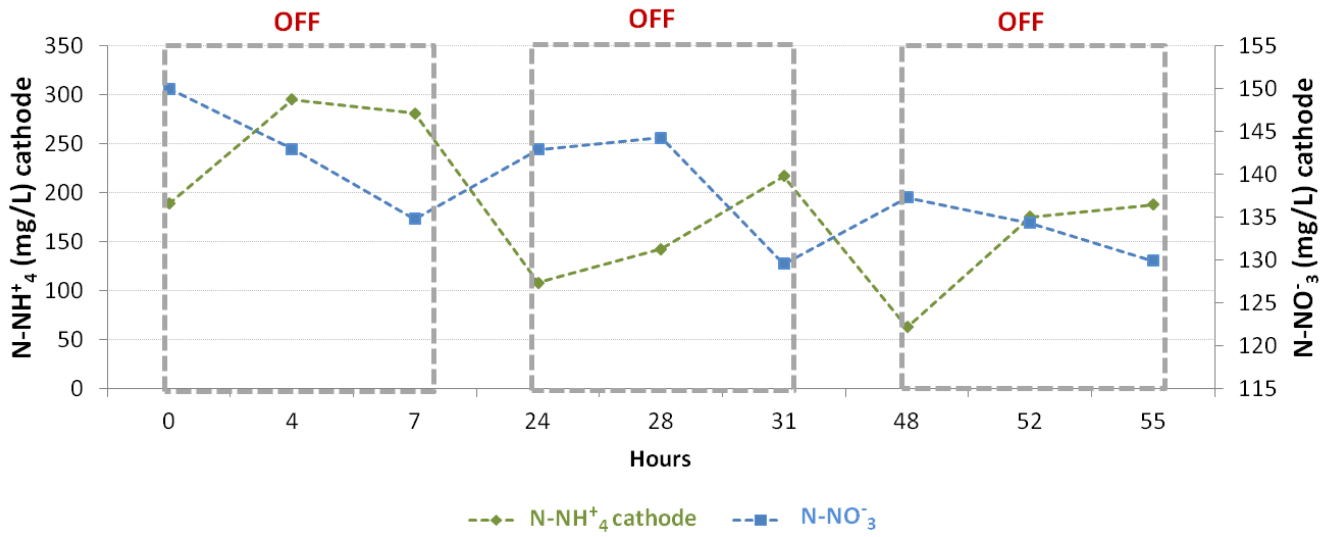
OFF
OFF
OFF
N-NH+4 (mg/L) cathode
N-NO-3 (mg/L) cathode
Hours
N-NH+4 cathode
N-NO-3

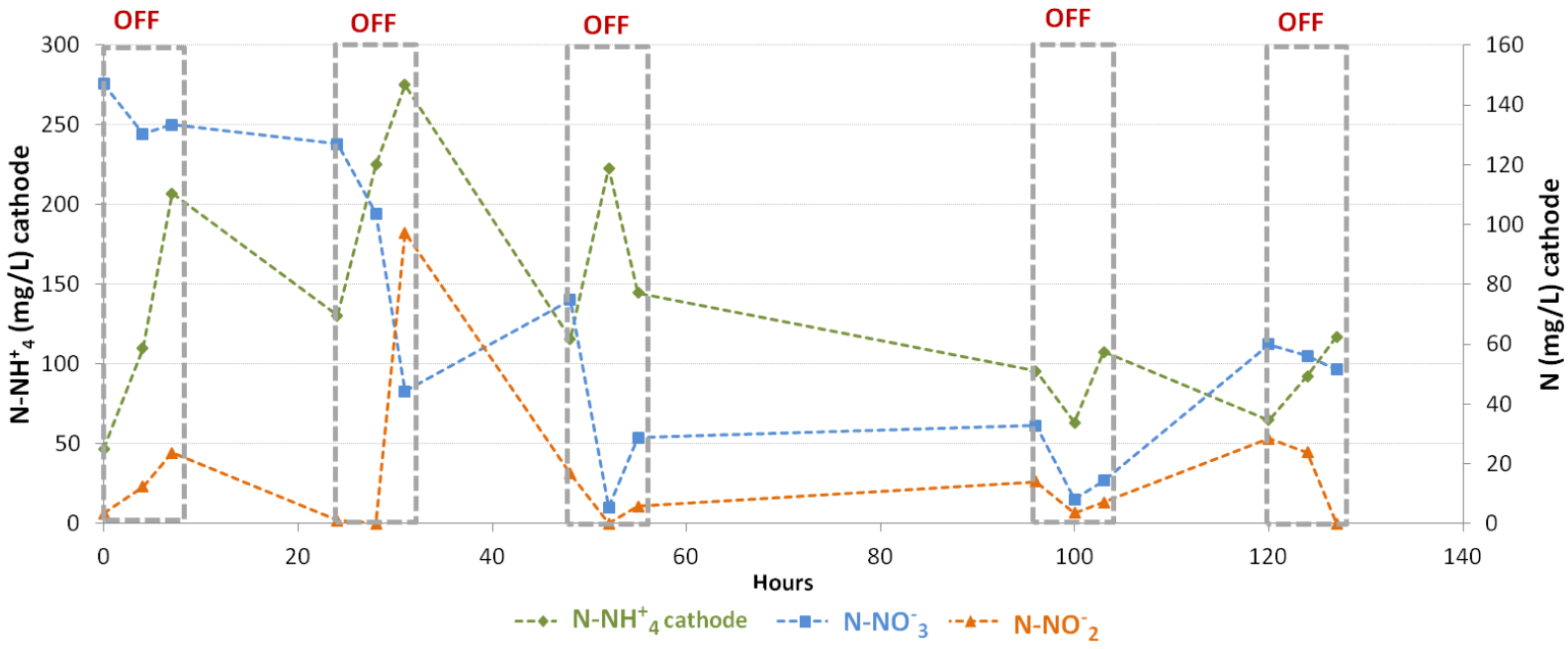
OFF
OFF
OFF
OFF
OFF
N-NH+4 (mg/L) cathode
N (mg/L) cathode
Hours
N-NH+4 cathode
N-NO-3
N-NO-2

Fig. 7

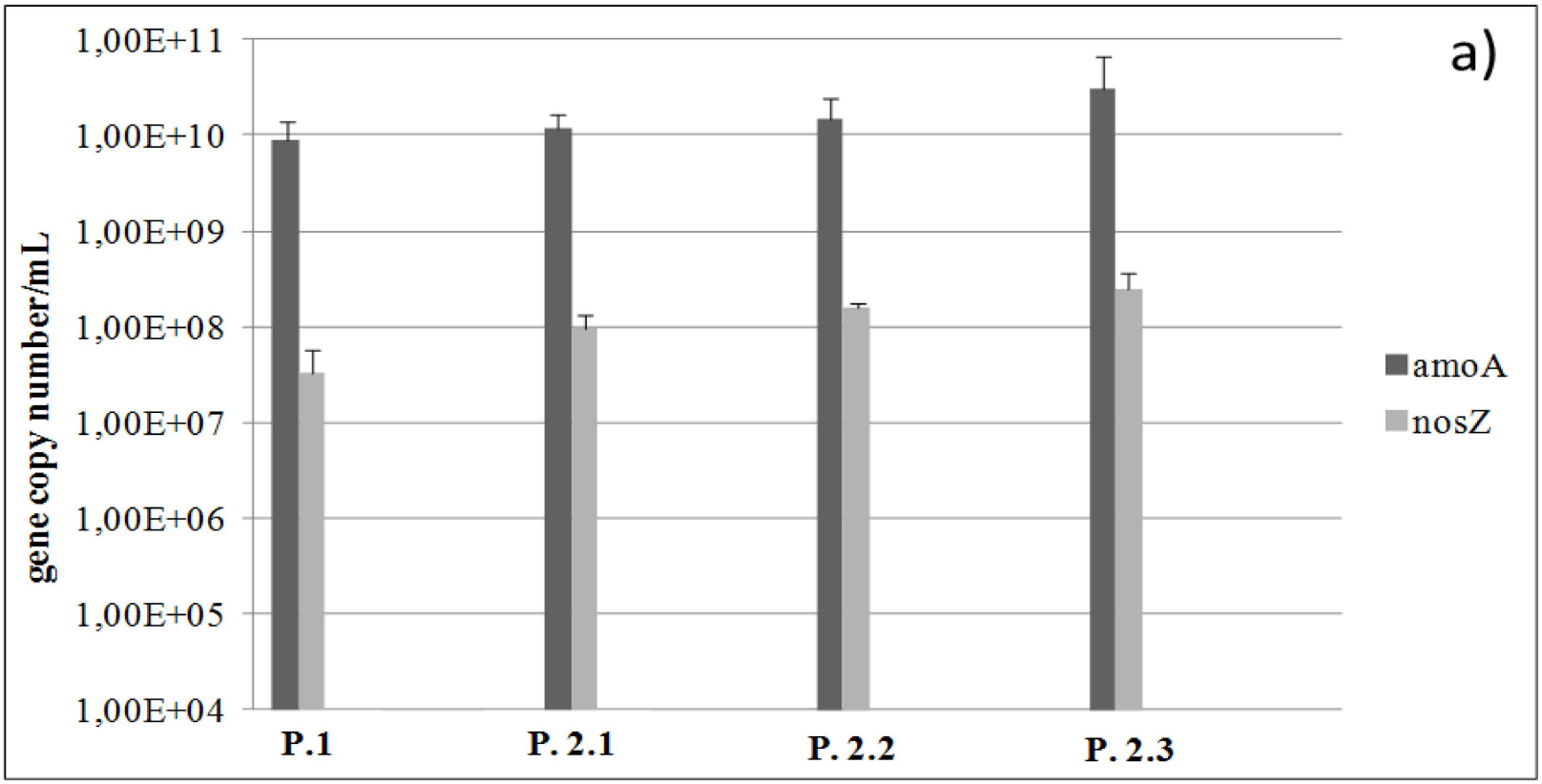

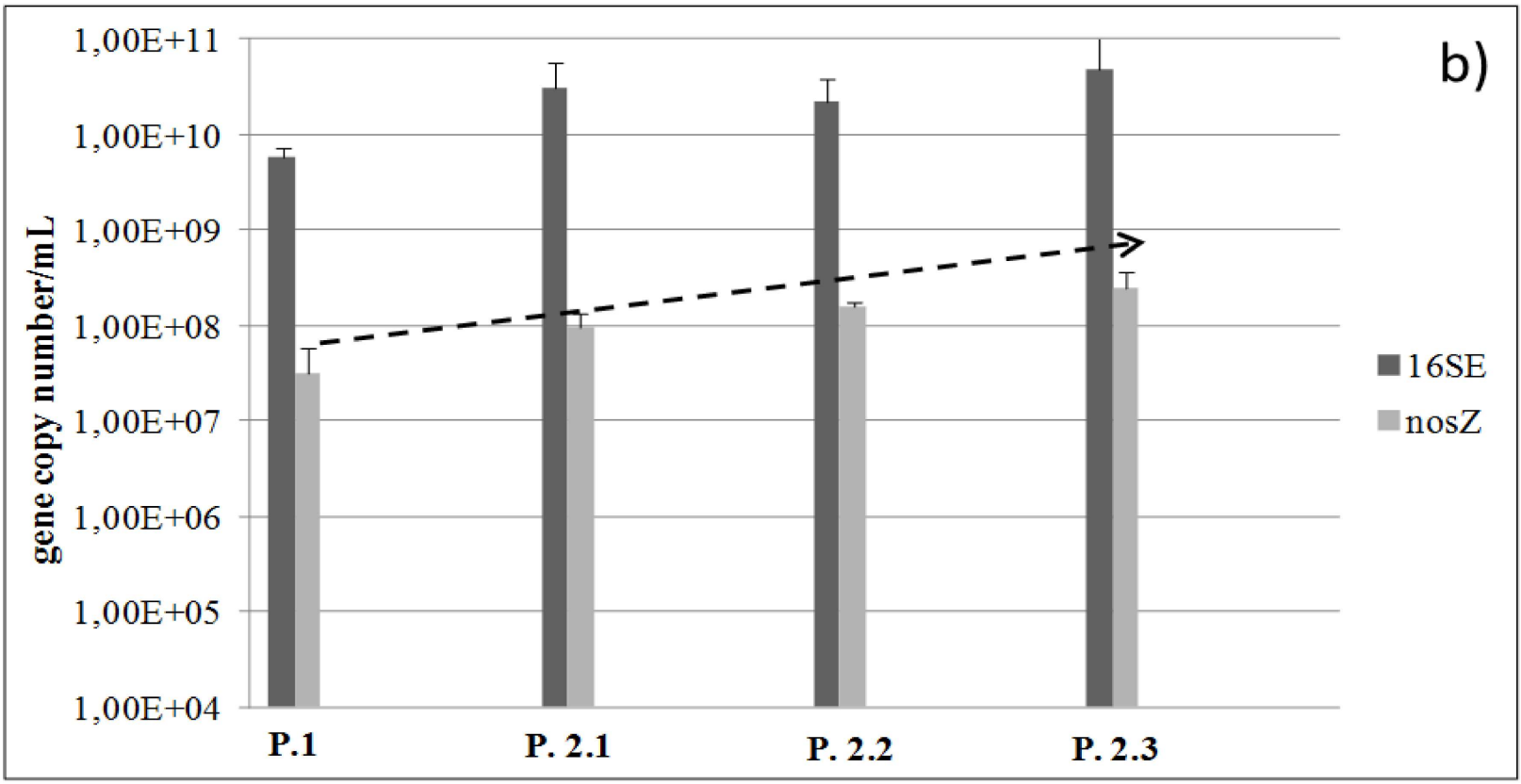

Aerated cathode

Intermittent aerated cathode

Intermittent aerated cathode + acetate